강섬유 보강 철근콘크리트 보의 재료적 에너지감쇠에 대한 실험 및 수치해석적 연구

Experiment and Numerical Investigation on Material Damping for Steel Fiber Reinforced Concrete Beams

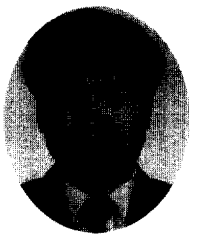

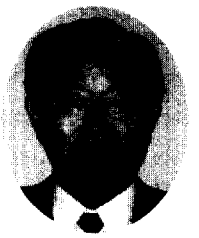

강보순* Kang, Bo-Soon

정영수** Chung, Young-Soo

이우현*** Lee, Woo-Hyun

요 약

동적하중하에서 강섬유보강 콘크리트(SFRC)는 유연도 및 균열억제에서 우수한 재료로서 최근에 각종 구조물에 널리 사용되고 있으며, 특히 내진설계를 위한 강섬유보강 콘크리트의 재료적 감쇠에 관한 규명이 절실히 요구되고 있다. 본 연구는 강섬유보강 콘크리트(SFRC)보의 재료적 감쇠효과증진을 실험적 및 수치해석적 방법으로 규명하는 데에 목적이 있으며, 일반적으로 강섬유보강 콘크리트(SFRC)보의 감쇠거동은 인장철근비, 강섬유의 혼입량과 형태, 콘크리트의 강도 그리고 응력의 크기에 좌우된다. 강섬유 보강 콘크리트보의 감쇠비는 보의 균열상태 변화에 따른 동적실험결과로부터 얻을 수 있으며, 일반적으로 강섬유보강 콘크리트는 증가된 에너지감쇠능력으로 인장철근이 소성전 상태에서 철근 콘크리트보의 경우보다 향상된 감쇠거동을 갖고 있는 것으로 판명되었다. 이들 결과의 수치해석적인 입증을 위하여 curvature(곡률)와 감쇠값사이의 관계를 기초로 유한요소프로그램(TICAL)을 개발하였으며, 결론적으로 0.44% 인장철근비를 갖고 있는 강섬유보강 콘크리트의 감쇠비는 하중상태에 따라 철근 콘크리트 보의 경우보다 약 5%에서 35%정도 향상된 감쇠비를 갖고 있는 것으로 조사되었다.

* 정회원, 중앙대학교 건설환경공학과 강사
** 정회원, 중앙대학교 토목공학과 교수
*** 중앙대학교 건설환경공학과 교수

·본 논문에 대한 토의를 1999년 2월 28일까지 학회로 보내 주시면 1999년 4월호에 토의회답을 게재 하겠습니다.

1. Introduction

Damping in reinforced concrete structures has been the subject of many researchers in the past [1],[2],[3],[4],[5],[6]. Dependency of damping wth respect to the performance load level and to the degree of damage has been the central subject from the experimental tests carried out by Dieterle and Bachmann[2]. Damping has been derived from the free vibration response curves as well as from the resonance response curves, and the characteristic behaviour has been separately identified.

Dieterle[2] distinguished two different test-phases (1.and 2.tests-phase). In each test-phase, the initial displacement increased from lower to higher values. The first phase represents the stage of developing cracks (Fig.1a) whereas the second phase represents the damaged beam (Fig.1b). It is observed that damping increases with larger initial displacement in the first phase (see Fig. 1a). The reason for this is the increasing frictional damping while cracks are developing. After all cracks are developed, because equivalent damping values resulting from frictional damping are decreasing with a higher initial displacement (see Fig.1a and Fig.1b).

The damping behaviour of reinforced concrete members has further been investigated by Heiland[5] and has been extended to steel fiber reinforced concrete members. The presence of steel fibers in the reinforced cement matrix significantly alters the frictional damping due to closing and opening of cracks through the

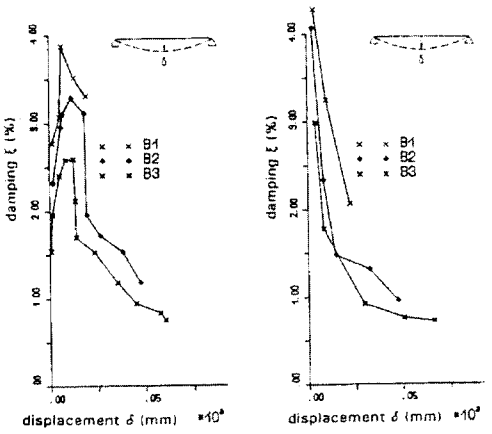

Fig.1 Damping behaviour of reinforced concrete at the first and second test-phase[2]

bonded steel fiber reinforcement within the cracks.

Damping derived from decaying response plots generally indicates the integral structural and material damping. It is only a quantitative figure and can vary according to the structural system. Considering this limitation, Heiland[5] attempted to derive the damping at element level, i.e. damping has been related to the curvatures of the element at a flexural deformed state. This kind of first study has been developed for both reinforced and steel fiber reinforced concrete members.

The material damping as a function of the curvatures has been implemented in a general finite element program at an element level. This method of analysis is helpful in obtaining global damping behaviour of structural system and can be compared with the measured experimental data.

In practice, the integral damping is considered as a constant irrespective of the magnitude of loading and the performance of individual structural members for ease in a numerical computation. Based on a hyperbolic variation of damping as a function of the displacements for a given initial displacement an equivalent constant value is derived, to improve the present practice [5].

2. Determination of system and element level damping

Fig. 2 shows the midspan deflection of a free oscillating RC beam with 1.6 Vol.% steel fibers. It is possible to analyse the data down to amplitude of approximately 0.1 mm. The system (global) damping can be determined from the experimental data of amplitude decay response and damping constant ξ_i is obtained from equation (1).

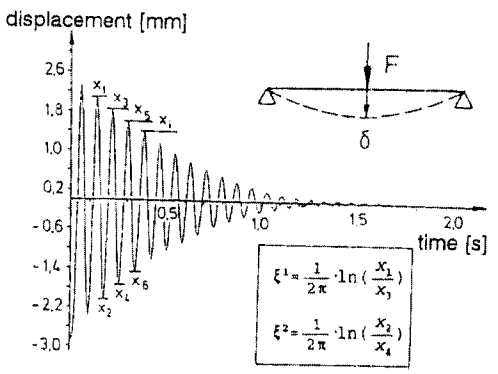

Fig.2 Free vibration experiment

$$\xi_{i,} = \frac{1}{2 \cdot \pi \cdot n} \cdot \ln\left(\frac{x_i}{x_{i+n}}\right) \qquad (1)$$

By deriving this damping constant for a structural member in practice, it is assumed that the damping value is constant at every cross section along the span of the structural member. But it is evident that the specific state of the cracks along the span has an important influence on the damping. Based on this "local concept", a method is illustrated to derive an element damping and not the commonly used system damping.

The total energy dissipation of a structural member under free vibration oscillations can be expressed as

$$D_{total} = \int D \cdot dv \qquad (2)$$

where D_{total} =Total damping of complete system

D =Damping in a volumeelement

Considering the member with n discrete elements, eq. (2) can be written as

$$D_{total} = \sum_{i=1}^{n} D_i \qquad (3)$$

D_i = dissipated energy in an element

Inserting the definition of Lehr's damping ratio

$$\xi_{i,} = \frac{1}{4\pi} \frac{D_i}{W_i} \qquad (4)$$

in eq. (3) we obtain:

$$\xi_{total} \cdot W_{total} = \sum_{i=1}^{n} \xi_i \cdot W_i \qquad (5)$$

Eq. (5) shows that the sum of the products of the equivalent viscous damping for an element with the respective element potential energy is equal to the total system energy dissipation.

Thus, the m-th element damping can be computed from

$$\xi_m = \frac{\xi_{total} \cdot W_{total} - \sum_{i=1}^{m-1} \xi_i \cdot W_i - \sum_{i=m+1}^{n} \xi_i \cdot W_i}{W_m} \qquad (6)$$

The energy stored in an element can be approximately expressed in terms of the respective average moment M_i and the curvature $\varkappa_i$ as

$$W_i = \frac{1}{2} \cdot \varkappa_i \cdot M_i \qquad (7)$$

Substituting eq. (7) in eq. (6) leads to:

$$\xi_m = \frac{\xi_{ges} \cdot \sum_{i=1}^{n} K_i \cdot M_i - \sum_{i=1}^{m-1} \xi_i \cdot K_i \cdot M_i - \sum_{i=m+1}^{n} \xi_i \cdot K_i \cdot M_i}{K_m \cdot M_m} \qquad (8)$$

By eq.(8) the damping in the m-th element can be computed based on (n-1) element damping. Based on this relation, the variation of damping with the curvature can be developed (Fig.10).

3. Experimental Investigation

All tests have been carried out on simply supported rectangular beams, each measuring 80x160 mm in cross section and 3000 mm in length (Fig.3). The beams were vibrated horizontally across the longitudinal axis: the stresses induced by dead weight are not coupled with oscillation.

They have been chosen so that the first natural frequency for uncracked conditions is below 15 Hz (as is to be observed in many structures). Furthermore the stress by dead weight are to be much less than the tensile strength of concrete. The actual frequency range between ≈14 Hz for the uncracked and ≈5 Hz for the cracked stage, and the edge stresses due to dead weight are about ± 1.0 N/mm^2.

A special device has been developed which horizontally deforms the beams to its initial deflection, avoiding any fixing agents on the beam. So there are no disturbances of the most strengthened middle region of the specimen. Futhermore it can be reused in every test. Instead of a mainly used tension anchor a compression bar was employed. First an outer situated setback spring is compressed, and turning the adjustment nut the bar moves the beam away from the abutment.

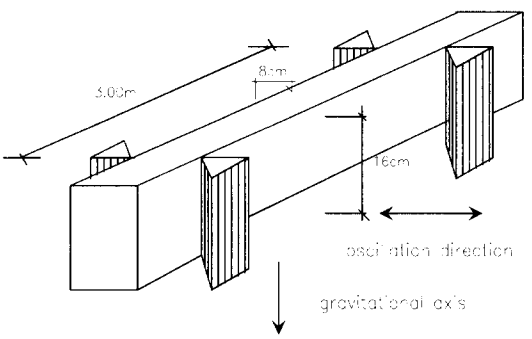

Fig.3 Test specimen

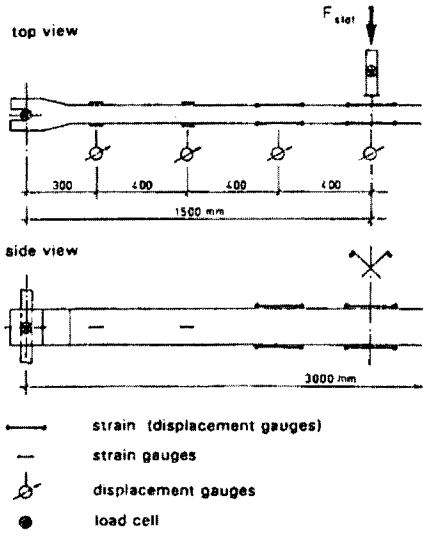

Fig.4 Measuring arrangement

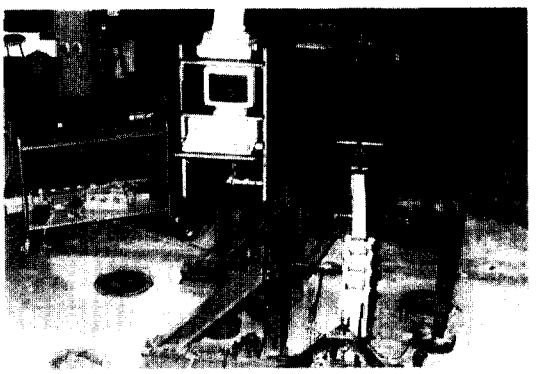

Fig.5 Photo of the test setup

The instrumentation used in the test program is shown in Fig.4. The basic parameters considered in this study were the volume of steel fiber, the percentage of longitudinal reinforcement and the strain controlled loading stages.

At first, the static load was imposed on the beam such that a predetermined deformed stage was obtained. By means of an on-line computer data processing program, the strains and the displacements in various elements of the beam at a respective load were known. After obtaining a strain controlled deformation state, the beam was set to oscillations by a sudden release of the load mechanism. The free vibration response data was collected for the computation of damping.

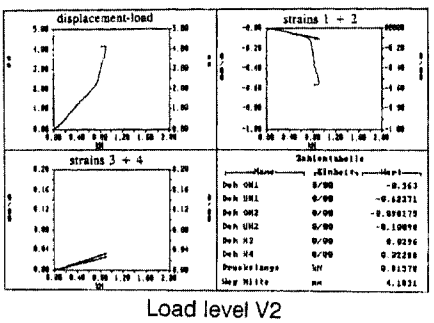

Fig.6 On-line computer programme output for elements 1 to 4

Table 1 Properties of test beams

Beam designation	Number of beams	Volume fraction of fibers Vf [%]	Type of fibers	Degree of tension reinforcement $\mu 01 = \mu 02$ [%]	Concrete strengt class by DIN 1045
B1	3	0.0	-	0.44	B 25
B2	3	0.8	straight	0.44	B 25
B3	3	1.6	straight	0.44	B 25
B4	3	0.0	-	1.23	B 25
B5	3	1.6	straight	1.23	B 25
B6	3	1.6	hookended	0.44	B 25
B7	3	0.0	-	0.44	B 45
B8	3	1.6	straight	0.44	B 45

Here the load stages have been identified with respect to the strains or a performance stage. Performance stage V1 was considered up to the stage of no initiation of cracks. The oscillations starting from this load stage were all in the range of a non-cracked state, consequently there was no significant difference in damping.

In the next performance stage V2, i.e. the beginning of cracks, could be identified with the characteristic increase of strains in the central element 1 as shown in Fig.6. With the help of on-line data processing, repeated vibration tests, could easily be performed at the same strain controlled load stage. Further increase of load levels caused new cracks which could be easily considered in the data processing and in the damping computation.

4. Results system and element damping values of RC and SFRC beams

The response from free vibration records shows that, for one curve the system (global) damping varies in a typical hyperbolic form having higher damping values at smaller amplitudes of oscillations. The position of a specific curve depends upon the initial maximum amplitude of the displacement imposed on the system for a free vibration response. In Fig. 7 five different performance controlled load stages (V2 to V6) responses are presented.

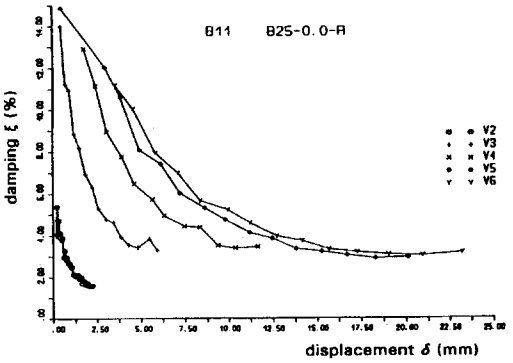

Fig.7 Damping versus displacement under different initial amplitude displacements

Based on these group of curves the upper and lower bounds of the variation of damping can be developed. The damping ordinates lying between these bounds, correspond to the given maximum displacement and actual response measured.

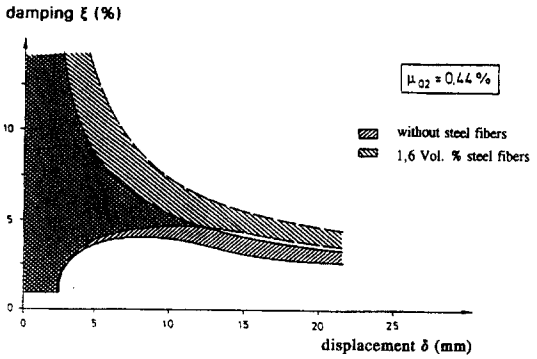

Fig.8 Influence of steel fibers in low reinforced concrete beams

Figures 8 and 9 show the response of low and highly reinforced RC and SFRC test beams. The presence of 1.6 Vol. % of steel fibers shows about 15% increase in the damping for low reinforced beams. As opposed to this the influence of 1.6 Vol. % of steel fibers in highly reinforced concrete beams is on the damping quasi insignificant.

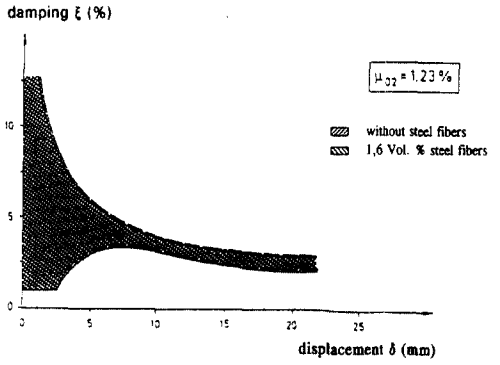

Fig.9 Influence of steel fibers in high reinforced concrete beams

Based on the experimental data, the derived element damping can be expressed with respect to curvature. Fig. 10 shows the damping-curvature relation for beams with and without steel fiber. This relation is valid irrespective of the location of the element and the boundary conditions of the structural member.

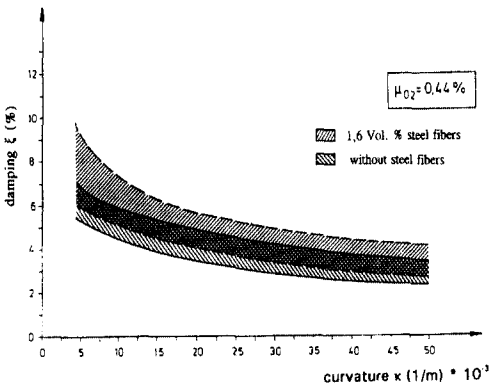

Fig.10 Variation of damping versus curvature

5. Numerical investigation

A FEM-program which considered the element damping as a function of the curvature (Fig. 10) and which took into account the bilinear moment-curvature relationship of RC and SFRC beams was developed.

The order of degrees of freedom of a beam element is shown in Fig. 11. The specimen is by 14 beam elements discretized.

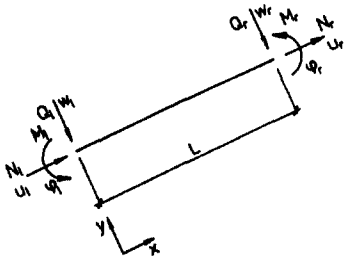

Fig.11 Order of degrees of freedom of a beam element

The relationship between the forces of a dynamically excited system is expressed as the following the differential equation in matrix:

$$[M]\{\ddot{U}\}+[C]\{\dot{U}\}+[K]\{U\}=\{F(t)\}$$

where [M] is the lumped mass matrix, [C] the damping matrix, [K] the stiffness matrix. $\{\ddot{U}\}$ is the nodal acceleration, $\{\dot{U}\}$ is the velocity and $\{U\}$ is the displacement vector, respectively.

a) The element mass matrix

$$M=\frac{\mu L}{420}\begin{array}{c|cccccc} & w_l & \psi_l & w_r & \psi_r & u_l & u_r \\ \hline & 156 & 122L & 54 & -13L & 0 & 0 \\ & & 4L^2 & 13L & -3L^2 & 0 & 0 \\ & & & 156 & -22L & 0 & 0 \\ & & & & 4L^2 & 0 & 0 \\ & & symmetric & & & 140 & 70 \\ & & & & & & 140 \end{array} \qquad (10)$$

b) The element stiffness matrix

$$K=\begin{array}{c} \begin{matrix} w_l & \phi_l & w_r & \phi_r & u_l & u_r \end{matrix} \\ \begin{vmatrix} \frac{12EI}{L^3} & \frac{6EI}{L^2} & -\frac{12EI}{L^3} & \frac{6EI}{L^2} & 0 & 0 \\ & \frac{4EI}{L} & -\frac{6EI}{L^2} & \frac{2EI}{L} & 0 & 0 \\ & & \frac{12EI}{L^3} & -\frac{6EI}{L^2} & 0 & 0 \\ & & & \frac{4EI}{L} & 0 & 0 \\ & \textit{symmetric} & & & \frac{EA}{L} & -\frac{EA}{L} \\ & & & & & \frac{EA}{L} \end{vmatrix} \end{array} \qquad (11)$$

c) The element damping matrix

Energy dissipation from viscous damping depends on the velocity and frequency of motion. Material damping is considered in the dynamic analysis when it is desirable to account for the dissipation of energy that exists in every real structure. Sometime it is introduced artificially as a means of suppressing the spurious oscillations in the numerical results.

Since the damping matrix could be either proportional to the mass or stiffness matrices as previously explained, a linear viscous damping matrix of the form

$$[C]=\alpha\cdot[M]+\beta\cdot[K] \qquad (12)$$

is usually employed, in which α and β are arbitrary proportionality factors. This is the well know Rayleigh-damping, which satisfies the orthogonality condition. It is therefore suitable to be used in the modal superposition solution technique. The major advantage of Rayleigh-damping is that no data storage need be allocated in the program to store the damping matrix.

The constants α and β may be assigned values using the relation

$$\xi_i=\frac{1}{2\cdot\omega_i}(\alpha+\beta\cdot\omega_i^2) \qquad (13)$$

if the damping ratio ξi, specified at two different frequencies ωi, is known. If ω 1 is the fundamental frequency of the system and ξi the desired damping ratio for the range of frequencies, another reasonable approach is to let ξi be equal to ξs at $\omega 1$ and evaluate αu and βu as

$$\alpha_u=\frac{2\cdot\xi_s\cdot\omega_1\cdot\omega_2}{\omega_1+\omega_2} \qquad \beta_u=\frac{2\cdot\xi_s}{\omega_1+\omega_2} \qquad (14)$$

The constants αu and βu of the Rayleigh-damping in the uncracked stage can be calculated as

$$\alpha=\alpha_u\frac{\xi}{\xi_s} \qquad \beta=\beta_u\frac{\xi}{\xi_s} \qquad (15)$$

in which αu and βu are the constants of the Rayleigh-damping in the uncracked stage, ξs the damping ratio in the elastic range, ξ the actual damping ratio in the cracked stage.

In (9) dynamic analysis of the structure is performed and, thus, the differential equation solved in the time domain, because then complex nonlinear properties can be taken into consideration. Implicit method is studied for this purpose and incorporated into a FEM-Program.

A implicit Method, the Newmark is chosen. This method has the advantage that results from (9) can still be obtained

with even large time increments; only for reasons of accuracy are small time steps to be used as a function of loading and the structure in question.

Comparisons of the experimental response and the numerical results are shown in Fig. 12. In general, the numerically predicted deflection of free oscillating beam for both load levels V1 (deflection δ max=2mm) and V6 (deflection δ max=25mm) generated with these material damping models are in very good agrement with the experimental results.

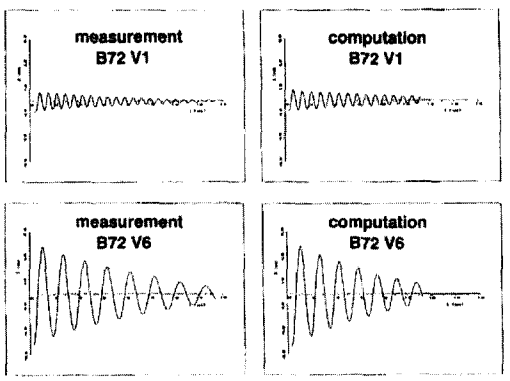

Fig.12 Comparisons of the experimental response and the numerical results

Fig. 13 and Fig. 14 compare the numerical predicted and experimental damping versus deflection curves for all load levels of beam with 1.6 Vol.% steel fibers. Again very satisfactory agreement is noted.

It is seen that in addition to determining the global damping behavior of a beam, here the damping behavior of an element of the beam is identified and introduced as damping versus curvature relation in a FEM-Program.

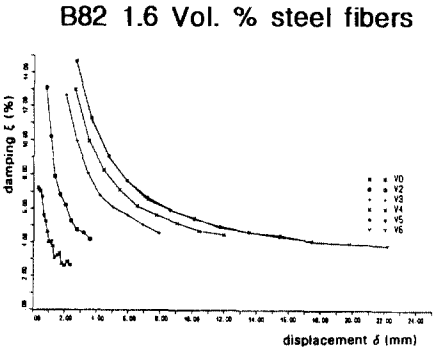

Fig.13 Numerical predicted damping versus deflection curves for B82

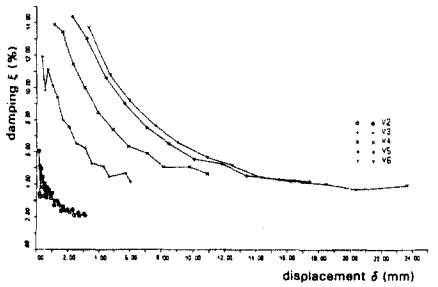

Fig.14 Experimental damping versus deflection curves for B82

The computed system damping values and the corresponding measured values are found to be in good agreement. [5].

In practice, it is preferred to have a uniform viscous damping value for all the performance stages of the structural members. Based on a hyperbolic variation of the damping with the displacement for a given initial displacement δ_2, an equivalent damping ξ_g was derived (by considering the equal areas in the response curve) as illustrated in Fig. 15. A comparison of such equivalent damping values (see Fig. 16) indicates, that there is a sufficient accuracy utilizing one constant damping value for all elements and performance stages. Execute calculations with such a constant damping value

resulted in a good approximation of the more sophisticated method.

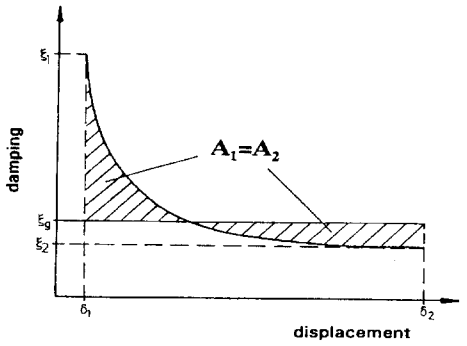

Fig.15 Determination the global damping versus value ξ g

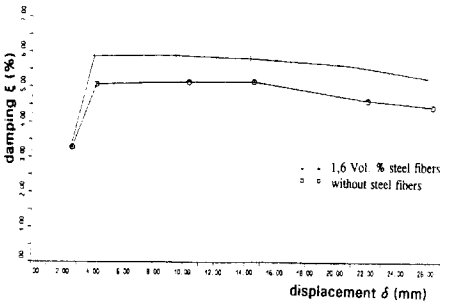

Fig. 16 Constant damping value initial displacement

6. Conclusion

Damping behavior of steel fiber reinforced concrete beam has been investigated by experimental and numerical method. The presence of 1.6 Vol % of steel fibers shows about 15% increase in the damping for low reinforced beams, but insignificant influence in the damping for highly reinforced concrete beams. Meanwhile, a FEM computer program has been newly coded on the basis of the relationships between curvature and damping of steel fiber reinforced concrete beams. The computed system damping values and the corresponding measured values are found to be in good agreement.

Reference

[1] Bock, E.: Über den dynamischen E-Modul u Dämpfung von Betonbalken verschied Bewehrung bei Biegungs-und Längsschwingun Dissertation, TH Berlin, 1939

[2] Dieterle, R., Bachmann, H.: Versuche üb Einfluss der Rissbildung auf die dynami Eigenschaften von Leichtbeton-und Betonb Bericht Nr. 7501-1, Inst. f. Bau u.Konstruktion ETH Zürich, Birkhäuser V 1979

[3] Lenk, H.: Über das Schwingungsverhalte Spannbeton-und Stahlbetonbalken. Dissertati Stuttgart, 1964

[4] Teichen, K.-T.: Über die innere Dämpfun Beton. Dissertation, Universität Stuttgart, 19

[5] Heiland, D.: Untersuchungen Dämpfungsverhalten von stahlfaserverstä Stahlbeton bei globaler und elementw differenzierter Betrachtungsweise, Disser Ruhr-Universität Bochum, 1991

6) Srinivasulu, P.: Lakshmanan, N.: Muthumani, K.: Sivarama Sarma, B.: Dynamic Behavior of Fiber Reinforced Concrete Beams. Proc. of the International Symposium on Fiber Reinforced Concrete, Madras, Indien, Dez.1987, 2.85-2.94

ABSTRACT

In this paper, damping behavior of steel fiber reinforced concrete(SFRC) beams by experimental and numerical method is discussed. Because of its improved ability to dissipate energy, SFRC has a better damping behavior than that of reinforced concrete(RC). Damping behavior is influenced by longitudinal reinforcement ratio, volume and type of steel fiber, strength of concrete and the stress level. Damping in the SFRC beams has been evaluated from dynamic experimental test data at various levels of cracked states in the beams. A FEM program(TICAL) has been developed based on the relationships between curvature and damping. It is observed for SFRC beams with 0.44% of tensile reinforcement steel that approximate 5% to 35% was relatively increased in the damping ratio generally depending on the load level.

(접수일자 : 1998.3.4)